Smart Structures and Systems, *Vol. 31*, *No. 2* (*2023*) *171-181*
https://doi.org/10.12989/sss.2023.31.1.171

Influence of asphalt removal on operational modal analysis of Egebækvej Bridge

Umut Yıldırım*

Department of Civil Engineering, Eastern Mediterranean University, Famagusta, North Cyprus, via Mersin 10, Turkey

(*Received September 13, 2022, Revised November 12, 2022, Accepted November 22, 2022*)

Abstract. Using the most up-to-date system identification methods in both time and frequency domains, the dynamic monitoring data from the reinforced concrete Egebaekvej Bridge near Holte, Denmark, is examined in this investigation. The bridge was erected in the 1960s and was still standing during test campaign before demolishing. The ARTeMIS Modal was adopted to derive the modal parameters from ambient vibration data. Several Operational Modal Analysis (OMA) approaches were applied, including Enhanced Frequency Domain Decomposition (EFDD), Curve-fit Frequency Domain Decomposition (CFDD), and Frequency Domain Decomposition (FDD). Afterward, Principal Component (SSI-PC), Unweighted Principal Component (SSI-UPC) Stochastic Subspace Identification methods were utilized. Danish engineering consulting company, COWI with the allowance of the bridge contractor BARSLUND, allow the researcher for this experimental test to demonstrate the impact of OMA applications.

Keywords: bridge testing; on site data collection; operational modal analysis; structural health monitoring

1. Introduction

The experimental modal analysis is not always practicable in several massive constructions, for instance, tall buildings, bridges, and towers. Usually, all these buildings vibrate when exposed to external loads that cannot be controlled on-site. On the other hand, OMA on-site relies on something distinct from the well-known input-output relationship for structure's response function as the excitation forces are vague. A so-called Gaussian white noise stochastic process is proposed to be driving the system's excitation, which indicates that an excitation load with identical energy degrees across all frequencies is stimulated evenly for full modes. Usually, this case does not reflect reality very well because specific inputs always have frequencies with higher energy than others. Accordingly, this situation is compensated by representing the unknown excitation loads using a linear filter to rightly formulate white noise with distributing energy over the involved bandwidth. Hence, broadband excitation is utilized to conduct OMA on the modes of interest.

Typically, loading forces tend to be more complicated as they are stochastic signals collection arising from the ambient excitations such as air disturbance, pedestrians, machinery and road or traffic vibrations. Monitoring civil infrastructure integrity was become a vital issue over the previous two decades, with related fields such as automated control, bridge or superstructure aging mastery, earthquake resistance, and cultural heritage preservation. Practically, structures may be monitored using vibrations based on the assumption that differences in the structural dynamic characteristics according to changes in a system's Eigen-structure, which can be quantified by using this method. Whelan *et al*. (2010) utilized subsequent structural identification with several instrumentation layouts to evaluate the global multi-span response of prestressed concrete bridge using roving sensors and reference-based techniques. OMA using ARMERA was applied of reinforced concrete bridge for damage detection in Park *et al*. (2016). The results in Yamaguchi *et al*. (2015) imply that damages in diagonal members of steel truss bridge could be detected from changes in modal damping of diagonal-coupled modes. Based on the modal properties extracted from the ambient vibration data, the initial finite element (FE) model of a bridge can be updated to represent the deflection of a bridge akin to the real value which can be easily obtained without measuring the real deflection (Yi *et al*. 2007). Ni *et al*. (2015) investigated the mode identifiability of the cable-stayed Ting Kau Bridge using ambient vibration measurements and the influence of the excitation intensity on the deficiency and robustness in modal identification. It is observed that a few low-order modes, including the second global mode, are not identifiable by common output-only modal identification algorithms under normal ambient excitations due to traffic and monsoon. The deficient modes can be activated and identified only when the excitation intensity attains a certain level (e.g., during strong typhoons). A series of field vibration tests are conducted on the Runyang Suspension Bridge during both the construction and operational stages. Based on the identified modal parameters, the effect of the pile-soil-structure interaction on dynamic characteristics of the suspension tower is investigated. It's found that

*Corresponding author, Ph.D., Professor,
E-mail: umut.yildirim@emu.edu.tr

ISSN: 1738-1584 (Print), 1738-1991 (Online)

compared with the identified results from the freestanding tower, the longitudinal and torsional natural frequencies of the tower in the tower-cable system have changed significantly, while the lateral mode frequencies change slightly. (Li *et al*. 2017).

Before modal parameter identification, a preliminary analysis should be carried out to understand the resonant frequencies of the bridge by using the *Spectral Density Estimations* which shows the frequency resolution of the *Spectral Density* (SD) diagrams, i.e., how many discrete equally spaced frequency lines in a range between zero frequency and the Nyquist frequency. The singular values of the matrices of the estimated SD function are shown by *Singular Value Decomposition* (SVD). At each frequency, there are as many singular values as there are measurements channels in the selected *Test Setup*. In the first stage, SVDs of the Power Spectral Densities (PSDs) were performed utilizing the FFD, EFDD, and CFFD procedures. In order to estimate the modal parameters of a single degree of freedom (SDOF) system, it was necessary to start with singular values close to the resonant frequency, which are proportional to the PSD of the system. Long recording intervals (> 60 minutes) were required to eliminate random, and leakage errors in PSD prediction, particularly for damping identification of the initial modes (beginning at 0.3 Hz), as previously reported. (Tamura *et al*. 2005, Uhlenbrock *et al*. 2006).

The SVD technique is employed to break down the spectral density functions matrix into singular values and vectors at each separated frequency in the FDD approach. The dominant mode appears at the first singular value spectrum and the others in different ones in every frequency. The EFDD technique is strongly correlated with the FDD, with just a few other methods to assess the damping and improve predictions of a system's frequencies and mode shapes. A reverse FFT is utilized to convert the SDOF spectral density functions to the time domain, leading to SDOF correlation functions for every system mode. Hence, the natural frequency prediction and the damping ratio can be computed using simple regression analysis. Fast Kurtosis Checking with a new frequency-domain, CFDD is variant of the EFDD approach. Using Kurtosis computations, a robust automated harmonic index was developed by Jacobsen (2006) and Jacobsen *et al*. (2007). Hence, a linear interpolation was applied to the SDOF functions obtained by the EFDD method to remove the harmonic components without destroying filtering. When a harmonic component was placed precisely at the peak of a structural model, the approach in Jacobsen *et al*. (2007) yielded decent outcomes besides might improve computing efficiency and accuracy.

Using SSI approach has been shown to be effective when fitting a linear algorithm to observations obtained from the system's input/output or output-only (Benveniste and Fuchs 1985, Peeters and De Roeck 1999, Van Overschee and De Moor 1996). With the raw measured time series as input, SSI approaches depend on linear least squares estimate of the model to get their results. This method was later developed for an extensive range of stochastic subspace algorithms in Döhler and Mevel (2011a, b), involving data-driven algorithms and covariance-driven such as SSI-UPC (Van Overschee and De Moor 1996). When utilizing this approach, defining the eigenvalues of poles computed from the available data is required. Because these poles are present, the estimation method concentrates on the modes, and any lower noise poles are returned with a natural frequency estimate that is much higher than the Nyquist frequency and a damping ratio of one hundred percent. In the visible frequency range, this technique results in pronounced stability of the number of modes indicated and the presence of almost no noise modes. Because of the extremely consistent prediction of the poles, the search for the best model order is no longer as important (Peeters and De Roeck 1999). The number of modes that could be discovered was much more significant than frequency domain approaches. Compared to the frequency domain techniques; a higher number of modes could be identified. Closely spaced and repeated modes may be used in conjunction with low or high dampening when using SSI methods. Since they operate in the time domain, there is no bias or frequency resolution paucity. Thereby, asymptotically accurate predictions of model parameters may be made. Additionally, since the SSI approaches are small algorithm order indicators, the statistical errors of the modal parameter are significantly low.

In this study, different OMA approaches were applied to identify the modal parameters from ambient vibration data. The monitoring survey on bridge structure allied to working plan of the contractor company, Barslund. Due to interruption in working schedule that caused cost overrun and delay for the deadline of demolishing and reconstruction process in addition with the inadequate number of sensors allocated from COWI (for example; used number of sensors used in Test-Undamaged-A and Test-Undamaged-B) directed researcher to conduct short periods of monitoring in limited time. During the test campaign period (each Test Setup duration was 15mins) the average temperature was between 13.88 and 17.22 degrees Celsius during Test-Undamaged-A and 18.88 and 20 degrees Celsius during Test-Undamaged-B, respectively. The surveillance of the temperature effects to the bridge structures needs long-term SHM instrumentation system that collect vibration and temperature data periodically. Therefore, the identified frequencies varied very slightly since the modulus elasticity of materials and support conditions did not change significantly for this value of rise in temperature. In view of that, temperature effects on bridge dynamic parameters were neglected for these short periods of monitoring surveys.

1.1 Structural information

Egebaekvej Bridge is a typical concrete bridge from the early 1960s. It was decided to replace it because the bridge did not meet the current requirements due to a traffic increase that has led to the construction of two extra traffic lanes. Consequently, a demolition is planned to broaden the additional highway lanes on both sides, as the current bridge spans too tiny. The lengths of the central spans are 12.85 m and 12.85 m. The two side spans are 10.85 m and

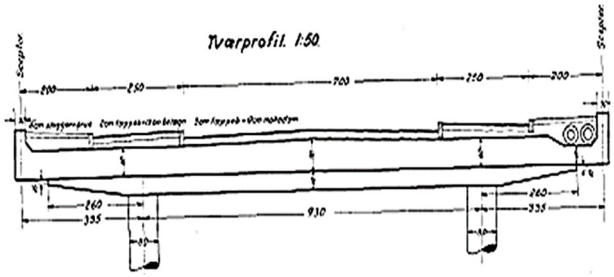

Fig. 1 Cross-section of the deck

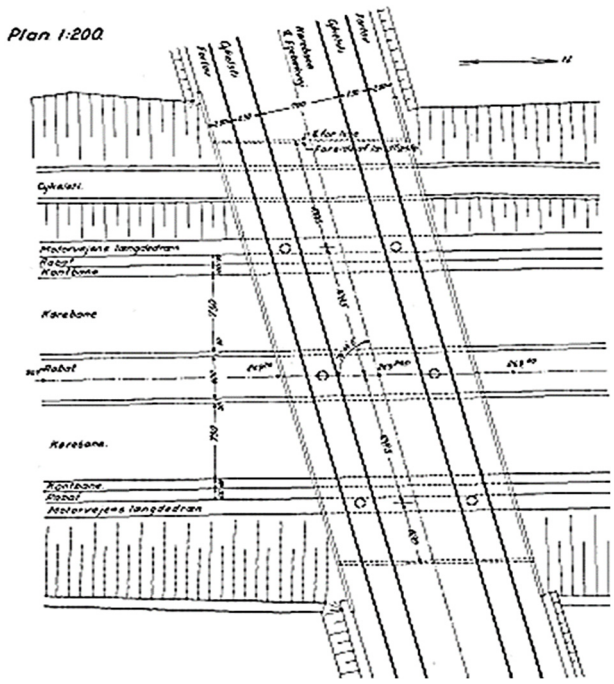

Fig. 2 Overview plan of Egebækvej Bridge

6.2 m long. The cross-section is 16 m wide and designed as a double layer reinforced slab that is ribbed 2.5 m in width and 0.4 m in thickness at girder-slab joints along the transversal direction of the deck. The cross-section of the deck and overview plan can be seen in Figs. 1 and 2.

2. In-situ test campaign

2.1 Campaign description

The primary objective of the current experimental test was to emphasize OMA under ambient vibration for the analysis of upcoming, removing asphalt layer and its effects on the parameters of the dynamic response in which this test was separated into two distinct segments. a) The bridge's current condition (*Test-undamaged-A*) was monitored during the first one, and the initial dynamic parameters were estimated. This experimental survey was taken place on 02/07/2013. b) During the second part (*Test-undamaged B*), the asphalt layer on the deck was removed on 05/07/2013. *Test-undamaged-A* was conducted in three steps (see Fig. 3) whereas *Test-undamaged-B* was conducted in two steps (see

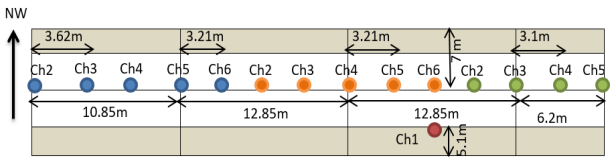

Fig. 3 Sensor layout of test-undamaged-A

Fig. 4 Experimental survey of test-undamaged -A

Fig. 5). Sensor placements and the pictures of an experimental survey on the site are seen in Figs. 4 and 6. Prepared raw data of the channels in Test Setup(s) were uploaded to the ARTeMIS Modal software. Later the channels from sensors are filtered, aliased, and positioned related to the d.o.f. and reference position (Ch.1) on the bridge's deck.

Several measurements were taken by moving sensors from one position to another. In this case, a small number of high-quality sensors are strategically positioned in locations where the probable modes of interest have a high level of response. These sensors, *reference sensors*, are fixed in the same position while shifting from one test setup to another. Other sensors are located in the single degree of freedom (DOF) positions for which the mode shapes are to be obtained. Generally, the mode shapes obtained of the moving sensors can be adjusted for different test setups to follow that of the *reference sensors* fixed to a specific position. It is worth noting that the *reference sensors* should be placed in such a way that the mode shape of the modes of interest has suitable amplitude in at least one of the references. Since locating a single position in which the amplitude is good can be difficult, it is recommended to utilize multiple reference sensors in various directions and positions. However, due to the limitation of the experimental facilities when conducting this study, a single

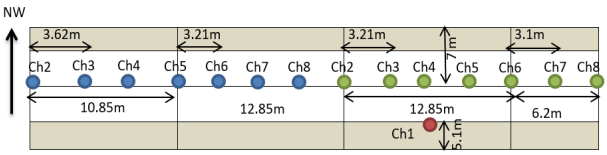

Fig. 5 Sensor layout of test-undamaged-B

Fig. 6 Experimental survey of test-undamaged-B

reference sensor was utilized. A test setup herein is referred to a scenario where available sensors are positioned, while a data set is a measurement obtained using a given *Test Setup*. Besides, in cases where the measurements are repeated for a particular *Test Setup*, they are referred to as new *Data Sets*. The analysis is conducted by using a single *Data Set* or merging multiple ones to generate longer records.

1.2 Data acquisition system and accelerometers

The used DAQ is a combination of 3 National Instruments 9233 (NI 9233), each of them has four-channel dynamic signal acquisition modules for making high-accuracy measurements from sensors. The four input channels simultaneously acquire at rates from 2 to 50 kHz. In addition, the modules include built-in antialiasing filters that automatically adjust to the sampling rate. Each simultaneous signal is buffered, analog pre-filtered, and sampled by a 24-bit delta-sigma ADC that performs digital filtering with a cut-off frequency that automatically adjusts to the data rate. The NI 9233 features a voltage range of ±5 V and a more than 100 dB dynamic range (see Fig. 7). The monitoring system consists of a network of 4513 002, IEPE accelerometers from Brüel&kjær (see Brüel&kjær website), able to acquire and record accelerations at different location across the bridge deck. Each *Test Setup* duration was 901.2 seconds.

Fig. 7 DAQ toolbox (NI 9233)

2.2 Measurement setup and signal processing

Once the measurements and geometry are assembled related to positions of sensors, the processing of the channels is begun by having the raw data copied to the processing section. After that, the data is standardized in which its meaning is eliminated. Moreover, the linear trend resulting from drift is removed by fitting each measurement channel to a first-order polynomial. Finally, the polynomial function is subtracted from the measurements. After then, decimation was employed to narrow the frequency range down to one with particular relevance. Indeed, in a frequency domain case, it is preferable to decimate to zoom in on the desired frequency band. Sampling frequency was 1968.5 Hz. Upper cut-off frequency of 49.21 Hz during the decimation of signal processing. The estimation of spectral densities was always performed with a resolution of 1024 discretization points (66% overlap) using a Hanning window.

3. Elaborations of monitoring

3.1 Parameter etimations

To derive resonant frequencies related to associated mode shapes and damping values, first, the FDD, EFDD, then CFDD (*primary analysis*) frequency domain-based analysis were conducted afterward, SSI-UPC and SSI-PC (*detailed analysis*) methods were utilized to verify and compare the accuracy of the estimated modes of the bridge.

For instance, Figs. 8-9 are the observed frequencies of *Test-Undamaged-A* including *Test Setup1*, *Test Setup2*, *Test Setup3* and *Merged Test Setups*, respectively. The frequencies obtained for each *Test Setups* by peak-picking from FFD diagrams later compared together with EFDD, and CFFD methods. SSI-UPC and SSI-PC stabilization diagrams are used to verify the resonant frequencies which are seen below the FFD diagrams in Figs. 8-9. Similar procedures are applied for *Test- Undamaged-B*. From Figs. 10-11, the obtained FDD peak-picking frequencies of *Test Setup1*, *Test Setup2* and *Merged Test Setup* are seen and compared together with the EFDD, and CFFD techniques alike for the *Test- Undamaged-A*. Later, SSI-UPC and SSI-PC stabilization diagrams are illustrated below the FFD plots in Figs. 10-11.

Table 1 Estimated frequencies and damping ratios

Case		Test-Undamaged-A								
Method		FFD	EFDD	CFDD	SSI–UPC1	SSI–UPC2	SSI–UPC3	SSI–PC1	SSI–PC2	SSI–PC3
F1 Torsinal mode	Frequency [Hz]	9.42	-	-	-	9.4	-	-	9.33	-
	Damping ratio (%)	0	-	-	-	6.12	-	-	6.24	-
F2 Torsinal mode	Frequency [Hz]	13.55	13.66	13.67	-	13.79	-	-	13.88	-
	Damping ratio (%)	0	1.49	1.182	-	3.88	-	-	3.77	-
F3 Torsinal mode	Frequency [Hz]	16.24	16.34	16.33	16.41	16.43	16.37	16.33	16.39	16.32
	Damping ratio (%)	0	2.03	1.04	2.23	1.85	3.65	1.86	2.44	1.01
F4 Torsinal mode	Frequency [Hz]	20.04	19.87	19.87	19.99	20.03	19.97	19.91	20.01	19.97
	Damping ratio (%)	0	2.68	1.66	2.92	3.92	3.335	2.76	2.06	3.24

In FDD plots, the modal domain where the modes found automatically (represented with a light green color in the back of the diagram), and the harmonic indicator (represented as vertical lines with a strong green color), and finally the modal coherence which is calculated by taking the first singular vector at the certain frequency and calculating the averaged dot products with the first singular vectors of the closest neighbouring frequencies (shown in light blue colors). Red dashed vertical lines defines the current estimator.

The observed frequencies from SSI methods were verified by the stabilization diagrams which shows *stable* modes in red dots, *noise* modes in brown dots and *unstable* modes in green dots. The green line defines the cursor model of the modes and pink line states the maximum eigen-frequencies chosen to estimate the number of modes. The singular values (the yellow horizontal bars) indicate the rank of the SSI input matrix to estimate a state space model and specify what subspace of singular values of this matrix to include in the estimation. This subspace should at least include all singular values significantly different from zero. As previously stated the identification of modal parameters was accomplished using the program ARTeMIS Modal.

3.1.1 Test-undamaged-A

As seen from *Test Setup1* primary analysis from FDD, four frequencies (11.77 Hz, 13.5 Hz, 16.48 Hz and 20.04 Hz) are observed distinctively related to modes of the bridge whereas only frequencies of 16.41 Hz, 19.99 Hz and 16.33 Hz, 19.91 Hz were observed from SSI-UPC and SSI-PC stabilization diagrams in vertical red dots, respectively (Fig. 8 (left)).

From the FFD diagram in Fig. 8 (right), the number of observed frequencies (9.42 Hz, 11.34 Hz, 13.69 Hz, 16.29 Hz and 20.04 Hz) in *Test Setup2* are higher than *Test Setup1* because of possibly sensor placements mounted on bridge internal midspans. Since, bridge internal midspans are more disposed to bending or torsional vibrations than the external spans. Nevertheless, the frequency of 11.34 Hz was not verified from in SSI-UPC and SSI-PC stabilization diagrams (see Fig. 8 (right)). The acquired frequencies seen in Fig. 8 (right; bottom) have low stability and thus higher dimension of eigenvalues was used to estimate the modes in SSI-PC stabilization diagram.

The *Test Setup3* shows that low intensity of ambient vibration was recorded during the test which are comprehended among the observed frequencies of 16.19 Hz and 20.09 Hz in Fig. 9(left). As a basic principle, lower amplitudes are permissible for higher frequencies. For example, lower frequencies are seen as noise modes but the higher frequencies from FDD diagram are corroborated from SSI-UPC and SSI-PC stability diagrams as seen in Fig. 9 (middle)-(bottom). Fig. 9 (bottom) showed that observed frequencies have low stability and again higher dimension of eigenvalues was used to estimate the modes in SSI-PC stabilization diagram. The sketch of EFDD and CFDD estimation plots are presented together with the FFD plot in Fig. 9 (top).

As a result, after merging all *Test Setups* for *Test-Undamaged-A*, the quantified observed frequencies (9.42 Hz, 13.55 Hz, 16.24 Hz and 20.09 Hz) are plotted and verified by the stabilization diagrams in Fig. 9 (right). As corresponding to FDD analysis SSI analysis validates the placement of perceived frequencies (see Fig. 9 (middle)-(bottom)). The estimated frequencies and damping ratios of *Test-Undamaged-A* are seen from Table 1.

3.1.2 Test-Undamaged-B

By way of realization from FDD analysis of *Test Setup1* in Fig. 11 (left), frequencies of 15.19 Hz, 17.69 Hz and 21.53Hz are particularly observed. The other observed frequencies which are repetitive could not be verified by the helping of stabilization diagrams in Figs. 11 (middle)-(bottom). There's a frequency observed around 18 Hz seen in Fig. 11 (bottom) which becomes noisy modes afterwards.

The perceived frequencies depicted in Fig. 11 (right) for *Test Setup2* are 10.57 Hz, 15.19 Hz and 17.73 Hz, respectively. The frequencies perceived are also seen from

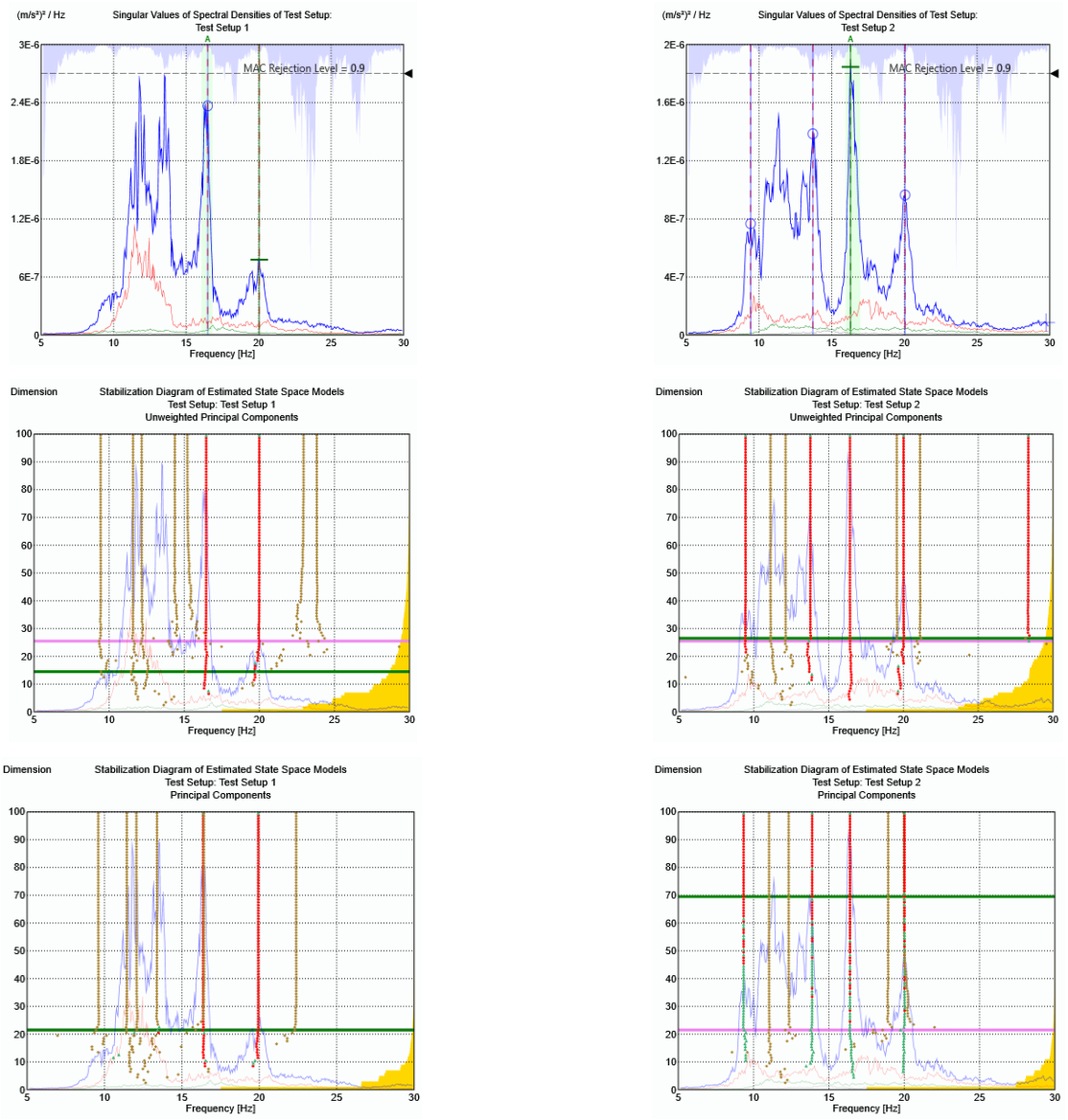

Fig. 8 FDD (top), SSI-UPC (middle), SSI-PC (bottom): left "*Test Setup1*"; right "*Test Setup2*"

the stabilization diagram in Fig. 11 (middle)-(bottom). The illustration of frequencies estimated by EFDD and CFDD methods are grasped in Fig. 11 (top) together with FDD method.

After amalgamation of all *Test Setups* for *Test-Undamaged-B*, the enumerated observed frequencies from FDD diagram are depicted and verified by the stabilization diagrams in Fig. 12. As parallel to frequency domain analysis time domain analysis gives compatible results and corroborates the placement of observed frequencies. The detected frequencies and damping ratios of *Test-Undamaged-B* are seen from Table 2.

3.2 Finite element modal analysis

The comparison was made between identifying the bridge's mode shapes utilizing experimental data from the deck (*Test-Undamaged-B*) and employing Finite Element Analysis (FEA). Finite Element Model (FEM) of the Egebakvej Bridge was created in SAP 2000 to serve as a reference for the OMA identification techniques for the *Test-Undamaged-B* (see Fig 10(a)). It is developed by as-built drawings, including frame components for columns and bents, shell parts for the concrete deck slab, and girder elements. The density of standard concrete material was assumed to be 2400 kg/m^3 and Young's modulus to be 2.48 10^{10} N/m, and the deck of the bridge was fixed at the abutments.

Figs. 10(b)-(e) indicate the first four modes generated by FEA. The captured frequencies from FDD diagrams and SSI-UPC stabilization plots for *Test-Undamaged-B* (asphalt and membrane layer removed) need to be well-thought-out carefully associating with computed natural frequencies of FEM. It is agreed from FEA that after the first two modes, torsional modes are dominant on the structure. Because the deck of the bridge is composed of only flat slab as a result, the structure is prone to transverse bending. The first two modes (7.54 Hz and 9.80 Hz) which are not caught by

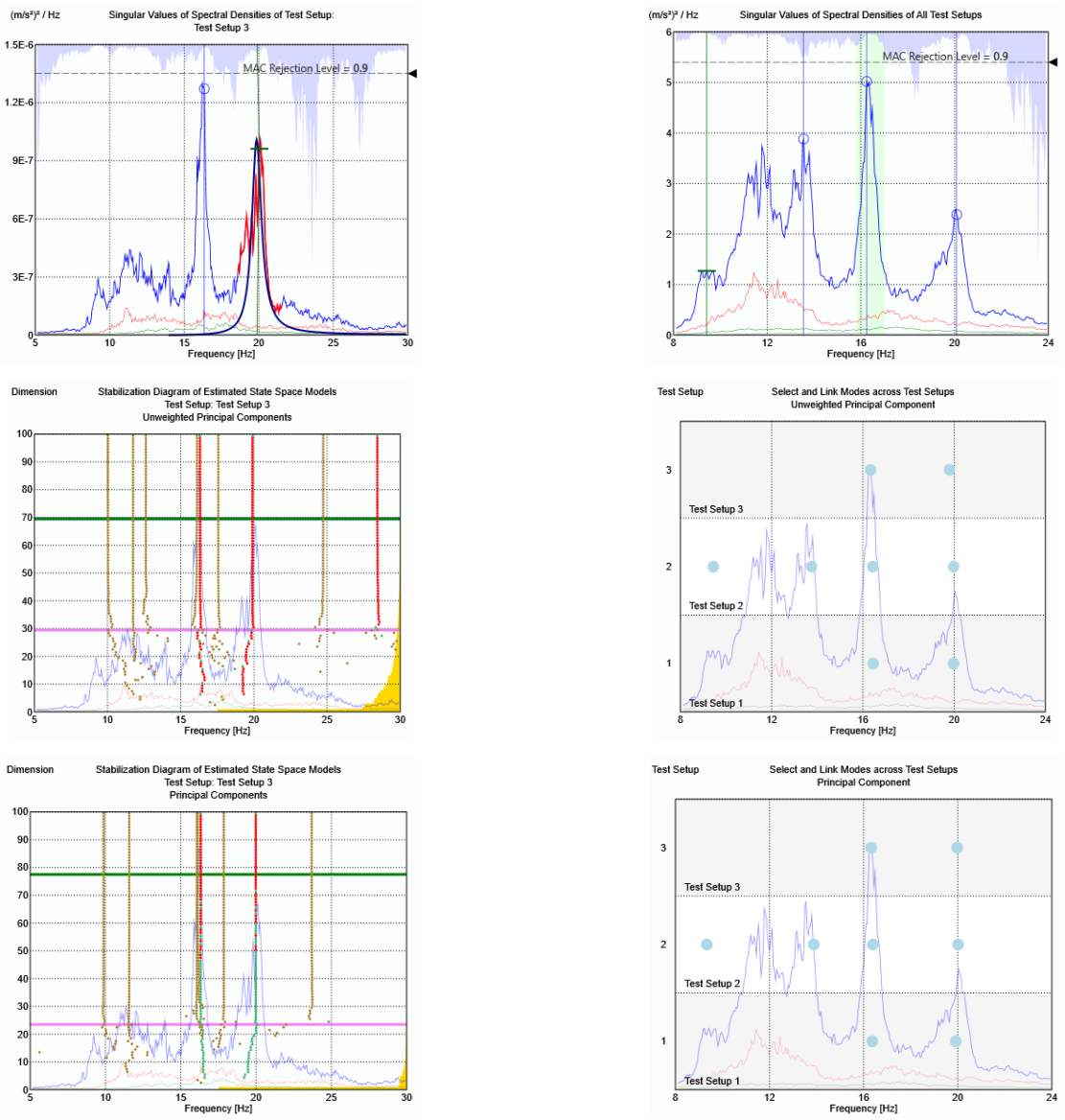

Fig. 9 FDD (top), SSI-UPC (middle), SSI-PC (bottom): left "*Test Setup3*"; right "*Merged Test Setup*"

Table 2 Estimated frequencies and damping ratios

Case		Test-Undamaged-A						
Method		FFD	EFDD	CFDD	SSI–UPC1	SSI–UPC2	SSI–PC1	SSI–PC2
F1 Torsional mode	10.57	-	-	-	10.47	-	10.38	-
	0	-	-	-	4.458	-	4.981	-
F2 Torsional mode	15.19	15.11	15.11	15.19	15.31	14.89	15.24	-
	0	1.295	0.717	2.988	2.874	1.337	2.628	-
F3 Torsional mode	17.73	17.74	17.73	17.69	17.87	17.65	17.87	16.33
	0	1.604	0.913	1.747	2.129	2.754	1.702	1.86
F4 Torsional mode	21.53	21.56	21.55	21.3	21.83	21.31	21.63	19.91
	0	2.103	1.275	3.05	2.778	3.67	3.108	2.76

OMA methods. Furthermore, it is comprehended that 4th mode is not exclusively captured from the FDD plot and repetitive frequencies are detected as noise modes in SSI stabilization diagrams (see Fig. 11). This might be triggered from the noise level (traffic, electric generator, etc.) around the test environment and the low length of raw data. It is

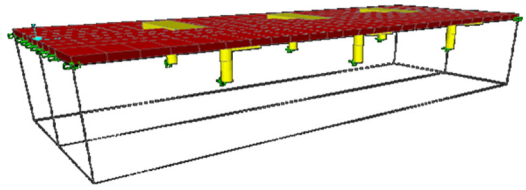

(a) FEM of Egebakvej Bridge

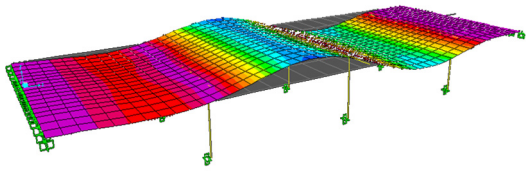

(b) 1st Mode of Egebakvej Bridge, 7.54 Hz

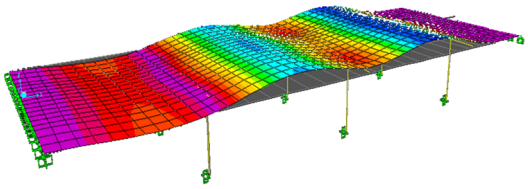

(c) 2nd Mode of Egebakvej Bridge, 9.80 Hz

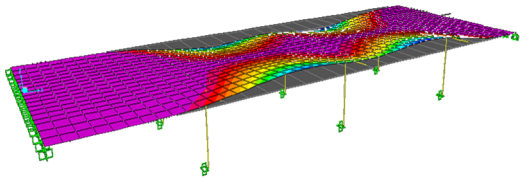

(d) 3rd Mode of Egebakvej Bridge, 10.52 Hz

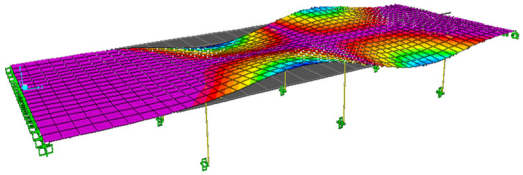

(e) 4th Mode of Egebakvej Bridge, 11.99 Hz

Fig. 10 FEM modal analysis

problematic to find the exact position for the modes of interest with good amplitude due to the one reference sensor and its position which was near to edge of deck. So, there are some frequencies, such as torsional, can be captured without difficulty on bridge deck regarding to the interaction of the type of ambient vibration mainly excited by the traffic jam.

3.3 Conclusive remarks

The estimated frequencies together with damping ratios regarding the usage of different kinds of frequency and time domain methods are presented in Tables 1 and 2, individually. The evaluated damping values along the bridge deck assesed related to the relevant observed modes of the bridge.

The observed frequencies which are extracted from the channels, characterize the operative dynamic stiffness of the bridge structure. The effects are seen in frequency spectrums, show a distinctive dynamic characteristic in both cases. The observed frequencies for *Test-Undamaged-A* are clearly visible within the frequency spectrums and matched with stabilization diagrams. The measurement observed from *Test Setup3* in *Test-Undamaged-A* has high level of noises and thus poor level in amplitude for lower frequencies. Once again, the last dataset observed from *Test Setup2* has high level of noises. The possible reason might be the placement of generator for electric supply which was becoming near to sensor positions during the last test surveys. Thus, increased high frequency level in test environment together with the high rapidity of traffic are permissible only higher frequencies. Therefore, the captured frequencies lower than 13.5 Hz and 15 Hz cannot be documented in frequency domain confidently for *Test-Undamaged-A* and *Test-Undamaged-B*, respectively. Moreover, the EFDD and CFDD methods as well give very high or low covariance to estimate the frequencies and damping ratios which are lower than 13.5 Hz and 15 Hz correspondingly for *Test-Undamaged-A* and *Test-Undamaged-B* as seen in Tables 1 and 2.

As seen from Tables 1 and 2, the bridge frequencies become higher after removing the asphalt and membrane layer. The captured frequency of 10.57 Hz obtained for the case of *Test-Undamaged-B* (asphalt and membrane layer removed) is consistent with the third mode (10.54 Hz) of FEA. The only problem here is the first two modes of FEM cannot be validated by OMA methods. It might supposedly be caused by the position of the reference sensor and the length of raw data (< 60 min). It is challenging to find the exact position for the modes of awareness with decent amplitude due to the one reference sensor. So, torsional frequencies of the bridge can be captured certainly regarding the interaction of the ambient vibration in this test surroundings. The fundamental resonant frequencies and accompanying bridge mode forms are influenced by traffic and may be detected in the upper-frequency range. The deck fundamental frequencies are located at upper frequencies owing to the mass and stiffness features of the bridge. The hapless thing is that as frequency increases, the degree of natural excitation drops, resulting in minor excited or weak modes compared to the bridge's primary frame.

Taking the advantage of the more sophisticated SSI methods together with EFFD and CFDD techniques, modal parameters are extracted. The damping values are a suitable indicator for the condition of the bridge deck. Damaged

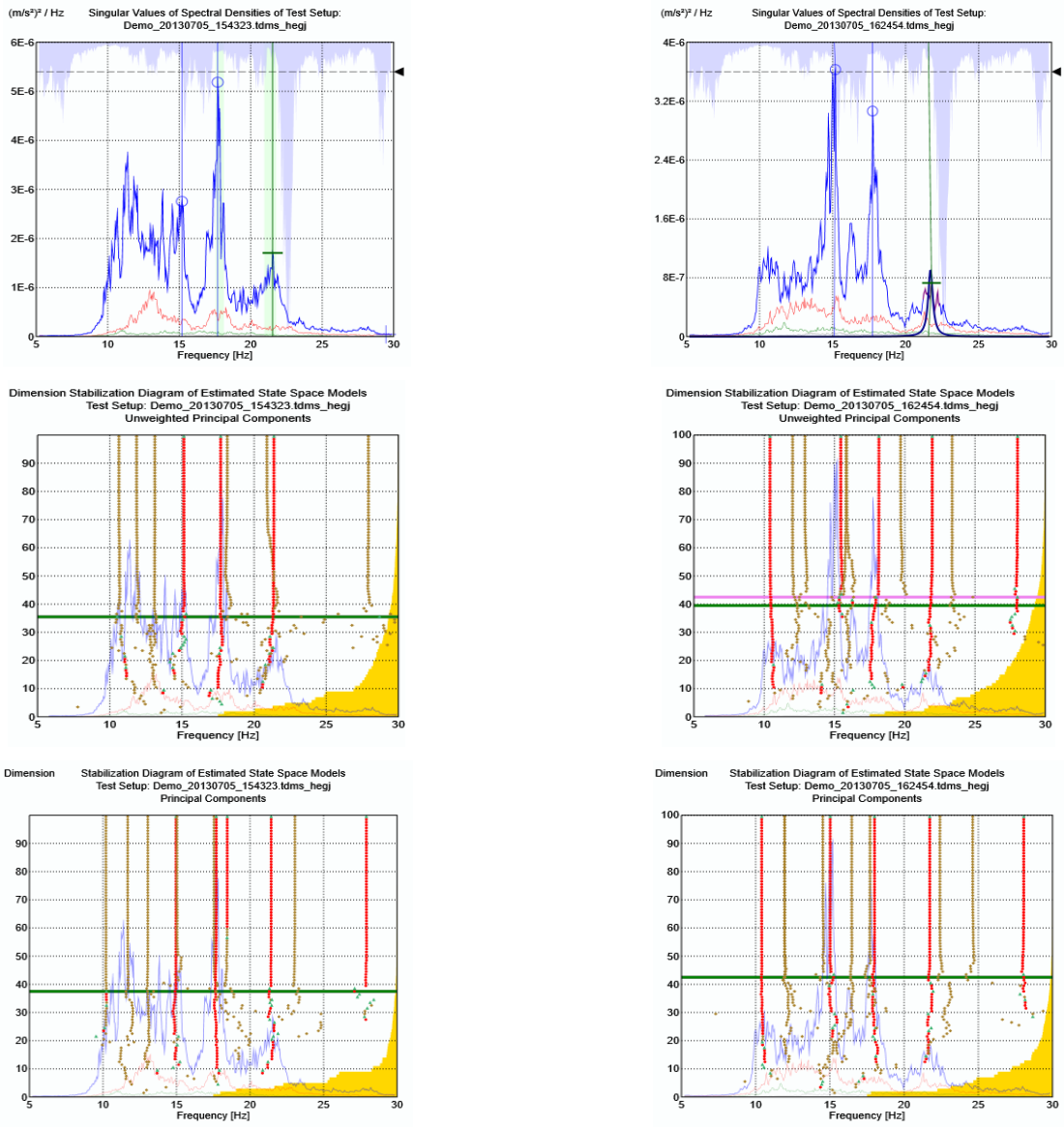

Fig. 11 FDD (top), SSI-UPC (middle), SSI-PC (bottom): left "*Test Setup1*"; right "*Test Setup2*"

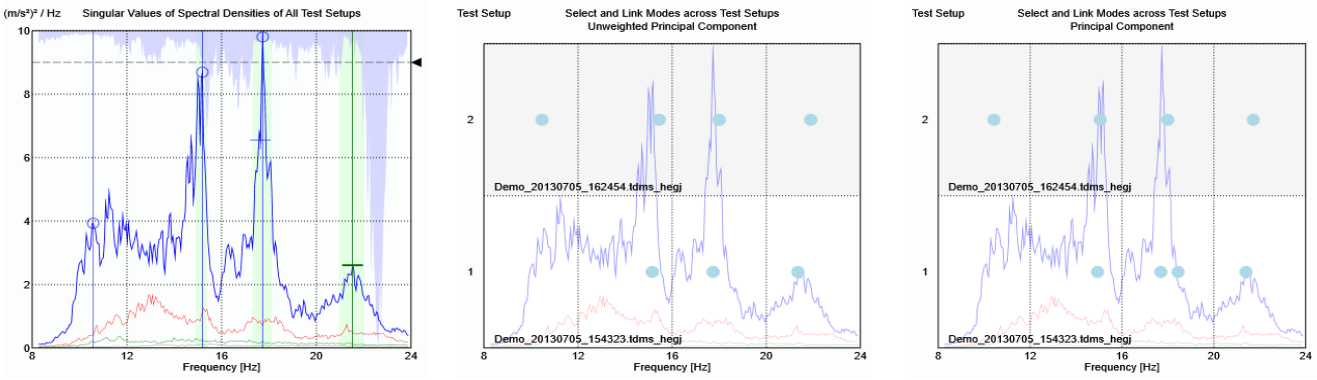

Fig. 12 FDD (top), SSI-UPC (middle), SSI-PC (bottom): "*Merged Test Setup*"

regions commonly dissipate energy in the form of friction which is reflected in an increase of the local damping values. Higher damping values are associated to abutments or piers which are structural frame based and thus have no straight effect on the assessment of the structure's condition. The pattern of damping values related to

captured modes for *Test-Undamaged-A* and *Test-Undamaged-B* show that the damping values are lessening when the asphalt and membrane layer removed. The damping values primarily reflects the system damping. Increased values from local spots according to material damping, which would point out certain damages (cracks, internal prestressing-problems), were not evaluated. Problems occurred identifying the damping and separating the mode shapes of repeated modes using first and secondary singular values. Partially this is caused by the incompleteness of the measurement model, especially for the lower frequency ranges.

4. Conclusions

The comparison between the *Test-Undamaged-A* and *Test-Undamaged-B* cannot easily be done because of the input energy level for adjusting the sensors response regarding to reference sensor. For that reason, the captured modes in both *Test-Undamaged-A* and *Test-Undamaged-B* are not easily compared in all frequencies. It is understood that generally the frequencies are increasing after removing the asphalt and membrane layers. Torsional modes are foremost than bending modes on bridge response which is understood from FEA. Because, the deck of the bridge is composed of only flat slab as a result the structure is prone to transverse bending.

OMA based system identification provides the following influential information for the bridge:

Dissemination of mass and stiffness properties related to observed frequencies.

a) Mass reduction due to removed asphalt layer is increasing the fundemetal frequencies.
b) Reduction of fastening joints at abutments due to removed asphalt layer affects the global stiffness and could possibly decrease the fundemental frequencies.
c) Temperature change which is not considered during the test survey. However, indetermined structural system moderately subject through to constraint by influence of temperature.

Significance of the induced vibration energy by means of damping along the bridge deck.

a) Reduction of damping due to removed asphalt and membrane layer is decreasing the damping ratio along the bridge deck for the associated modes.

It is agreed that practical test experience, type and level of stochastic (ambient) vibrations, reference sensor positions and the length of acquired data are crucial factors when OMA techniques are applied for the detection of structural dynamic parameters. Usage of OMA is an efficient tool for predicting modal parameters in bridge-type structures and is beneficial for scientific and practical applications in the industry.

In recent years, parametric (SSI) or nonparametric (FDD, EFFD, CFDD) automated smart OMA algorithms have been advanced and still developing especially for real time bridge monitoring and management systems. Parametric methods are generally of greater valuation precision but more complex and time overriding than nonparametric techniques. The automated SSI approaches are generally based on a variety of clustering algorithms with the goal of spontaneously inferring stabilization diagrams for modal identification and tracking of modes along with great precision on damping estimates. However, they comprise unknown input parameters while choosing high model order in order not to avoid missing physical modes within the considered frequency range. Latter over-specified system model order at the outlay of introducing spurious (noisy) modes are needed to be cleaned, classified or excluded. Therefore, a variety of unlike thresholds or clustering methods should be used for the parameters which are required to build clusters of unique modes for different eigenvalues and corresponding modes. These thresholds or parameters for clustering procedures are challenging to determine and confirm that no physical modes are removed and most of the spurious modes are cleaned. Since modal parameter estimators can be influenced in the presence of noise, the clusters based on these estimates can also be assumed to be biased.

The nonparametric methods are very direct for modal estimation but has a deficiency because of the limited frequency resolution. The automated nonparametric approaches mainly based on FDD for describing the refinement and identifying the spectral peaks automatically. Some other techniques employed a bandwidth identification step according to modal assurance criterion (MAC) sequences before the FDD process to identify physical peaks, and also proposed a modal tracking approach constructed on the spatial filtering. The other automated approaches based on the modal parameters of which are usually identified by single degree of freedom models like in EFDD or CFDD fitting method.

Currently; for smart bridge monitoring and management systems, Machine Learning (ML) and Artificial Neural Networks (ANN) based clustering algorithms are very promising within the automated OMA approaches to determine better classification of the physical unique modes.

Acknowledgments

Special thanks to Danish Road Agency for giving permission to use data and also Dr. Jacob Egede Andersen with Dr. Isaac Farreras Alcover from COWI with the purpose of conducting test campaign.

References

ARTeMIS (2022), Ambient Response Testing and Modal Identification Software ARTeMIS Modal v7.2; Structural Vibration Solution A/S Aalborg East. Denmark. www.svibs.com

Benveniste, A. and Fuchs, J.J. (1985), “Single sample modal identification of a non-stationary stochastic process”, *IEEE Transact. Automat. Control*, AC-30(1), 66-74. https://doi.org/10.1109/TAC.1985.1103787

Benveniste, A. and Mevel, L. (2007), “Nonstationary consistency

of subspace methods", *IEEE Transact. Automat. Control*, **52**(6), 974-984. https://doi.org/10.1109/TAC.2007.898970

Brüel&kjær, https://www.bksv.com/media/doc/bp2065.pdf

Döhler, M. and Mevel, L. (2011a), "Robust subspace based fault detection", *Proceedings of the 18th IFAC World Congress*, Milan, Italy, August.

Döhler, M. and Mevel, L. (2011b), "Modular subspace-based system identification from multi-setup measurements", *Proceedings of the 50th IEEE Conference on Decision and Control*, Orlando, FL, USA, December.

Jacobsen, N.-J. (2006), "Separating structural modes and harmonic components in operational modal analysis", *Proceedings of the IMAC XXIV Conference*, St Louis, MI, USA, January.

Jacobsen, N.-J., Andersen, P. and Brincker, R. (2007), "Eliminating the influence of harmonic components in operational modal analysis", *Proceedings of the IMAC XXV Conference*, Orlando, FL, USA, February.

Li, Z., Feng, D., Feng, M.Q. and Xu, X. (2017), "System identification of the suspension tower of Runyang Bridge based on ambient vibration tests", *Smart Struct. Syst.*, *Int. J.*, **19**(5), 523-538. https://doi.org/10.12989/sss.2017.19.5.523

Mevel, L., Basseville, M., Benveniste, A. and Goursat, M. (2002a), "Merging sensor data from multiple measurement setups for nonstationary subspace-based modal analysis", *J. Sound Vib.*, **249**(4), 719-741. https://doi.org/10.1006/jsvi.2001.3880

Mevel, L., Benveniste, A., Basseville, M. and Goursat, M. (2002b), "Blind subspace-based eigenstructure identification under nonstationary excitation using moving sensors", *IEEE Transact. Signal Process.*, SP-50(1), p. 41-48. https://doi.org/10.1109/78.972480

Ni, Y.Q., Wang, Y.W. and Xia, Y.X. (2015), "Investigation of mode identifiability of a cable-stayed bridge: comparison from ambient vibration responses and from typhoon-induced dynamic responses", *Smart Struct. Syst.*, *Int. J.*, **15**(2), 447-468. https://doi.org/10.12989/sss.2015.15.2.447

Park, K., Kim, S. and Torbol, M. (2016), "Operational modal analysis of reinforced concrete bridges using autoregressive model", *Smart Struct. Syst.*, *Int. J.*, **17**(6), 1017-1030. https://doi.org/10.12989/sss.2016.17.6.1017

Peeters, B. and De Roeck, G. (1999), "Reference-based stochastic subspace identification for output-only modal analysis", *Mech. Syst. Signal Process.*, **13**(6), 855-878. https://doi.org/10.1006/mssp.1999.1249

Reynders, E., Pintelon, R. and De Roeck, G. (2008), "Uncertainty bounds on modal parameters obtained from stochastic subspace identification", *Mech. Syst. Signal Process.*, **22**(4), 948-969. https://doi.org/10.1016/j.ymssp.2007.10.009

Tamura, Y., Yoshida, A., Zhang, L., Ito, T., Nakata, S. and Sato, K. (2005), "Examples of modal identification of structures in japan by fdd and mrd techniques", *Proceedings of the 1st IOMAC*, Copenhagen, Denmark, April.

Uhlenbrock, S., Rosenow, S.-E. and Schlottmann, G. (2006), "Application of Operational Modal Analysis to Marine Structures", *IOMAC Workshop*, Aalborg, Denmark, May.

Van Overschee, P. and De Moor, B. (1996), "Subspace Identification for Linear Systems: Theory, Implementation, Applications", Kluwer Academic Publishers, NY, USA.

Whelan, M.J., Gangone, M.V., Janoyan, K.D., Hoult, N.A., Middleton, C.R. and Soga, K. (2010), "Wireless operational modal analysis of a multi-span pre-stressed concrete bridge for structural identification", *Smart Struct. Syst.*, *Int. J.*, **6**(5), 579-593. https://doi.org/10.12989/sss.2010.6.5_6.579

Yamaguchi, H., Matsumoto, Y. and Yoshioka, T. (2015), "Effects of local structural damage in a steel truss bridge on internal dynamic coupling and modal damping", *Smart Struct. Syst.*, *Int. J.*, **15**(3), 523-541. https://doi.org/10.12989/sss.2015.15.3.523

Yi, J., Cho, S., Koo, K., Yun, C., Kim, J., Lee, C. and Lee, W. (2007), "Structural performance evaluation of a steel-plate girder bridge using ambient acceleration measurements", *Smart Struct. Syst.*, *Int. J.*, **3**(3), 281-298. https://doi.org/10.12989/sss.2007.3.3.281

FC